Structural and Functional Aspects of RGD-Containing Cyclic Pentapeptides as Highly Potent and Selective Integrin $\alpha_V\beta_3$ Antagonists

Roland Haubner,[†] Rainer Gratias,[†] Beate Diefenbach,[‡] Simon L. Goodman,[‡] Alfred Jonczyk,[‡] and Horst Kessler*[,†]

Contribution from the Institute of Organic Chemistry and Biochemistry, Technische Universität München, Lichtenbergstrasse 4, D-85747 Garching, Germany, and Merck KGaA Preclinical Research, Frankfurter Strasse 250, D-64271 Darmstadt, Germany

Received February 5, 1996[⊗]

Abstract: The $\alpha_V\beta_3$ integrin is implicated in human tumor metastasis and in angiogenesis. The design of low-molecular-mass $\alpha_V\beta_3$ antagonists by "spatial screening" led to the highly active peptides c(RGDFV) and c(RGDFV). Here the influence of the amino acids in positions 4 and 5 flanking the RGD-sequence on the inhibition of vitronectin and fibrinogen binding to the isolated $\alpha_V\beta_3$ and $\alpha_{IIb}\beta_3$ receptors was investigated. The influence of the side chain and the backbone conformation on activity and selectivity was studied. The compounds were divided into conformational classes. For each class at least one representative peptide was subjected to detailed structure determination in solution. The peptides of classes 1, 2, and 3 show a βII′/γ-turn arrangement with the D-amino acid in the $i + 1$ position of the βII′-turn. By contrast, the peptides of class 4 reveal a modified βII′/γ-turn pattern with glycine in the $i + 1$ position of the βII′-turn and the D-amino acid in the $i + 1$ position of the γ-turn. Class 1 is divided into two subclasses: besides the βII′/γ-turn arrangement a γ/γ-turn motif is found for two members of this class. Structure−activity relationship (SAR) investigations show that the amino acid in position 4 and the proton of the amide bond between residues 3 and 4 are essential for high biological activities toward $\alpha_V\beta_3$. By contrast, the amino acid in position 5 has no influence on the activity. A bent conformation of the RGD-sequence, as observed for the peptides of classes 1 and 2, fits the $\alpha_V\beta_3$ better than the $\alpha_{IIb}\beta_3$ receptor and so increases the selectivity of these peptides.

Introduction

Tumor metastasis is a major problem in cancer therapy. Cell−cell as well as cell−matrix adhesive interactions play important roles in this complex process.[1] In addition, the extravasated tumor must be able to grow in foreign tissue.[1,2] The development both of metastasis and of the primary tumor depends on nutrient supply, so finally the tumor-induced angiogenesis becomes important for the further development of the cancer.[3]

Integrins are cell surface receptors which are involved in adhesive interactions during the metastatic cascade. Integrins which establish tight contacts during tissue organization (e.g. $\alpha_2\beta_1$, $\alpha_5\beta_1$) may be down regulated in tumor cells.[4] On the other hand integrins involved in cell migration may be up regulated, e.g. the $\alpha_V\beta_3$ integrin is up regulated during the vertical growth phase and metastasis of malignant melanoma cells.[5] This integrin also plays a critical role in angiogenesis. The endothelial cells bind via the $\alpha_V\beta_3$ integrin to extracellular matrix components. In tumor tissue the inhibition of this interaction induces apoptosis of the proliferative angiogenic vascular cells.[6]

Metastasis[7] of several tumor cell lines and tumor-induced angiogenesis[6,8] can be inhibited both by antibodies that block integrin function and by small synthetic peptides acting as ligands for these receptors. The major advantages of small cyclic peptides are their easy, automatable synthesis, their resistance against proteolysis, and their weak immunogeneity. Many integrins can be inhibited by small peptides that possess the Arg-Gly-Asp sequence as a common receptor recognition motif.[1a,9] Incorporation of this sequence in cyclic penta- and hexapeptides containing D-amino acids, in a systematic manner, resulted in highly potent and selective inhibitors of integrins.[10] For the "spatial screening procedure" a sequence of amino acids is shifted around a cyclic peptide backbone structure by introducing the preferred conformation via their amino acid

[†] Technische Universität München.

[‡] Merck KGaA Preclinical Research.

[⊗] Abstract published in *Advance ACS Abstracts,* August 1, 1996.

(1) (a) Hynes, R. A.; Lander, A. D. *Cell* **1992**, *68*, 303−322. (b) Terranova, V. P.; Hujanen, E. S.; Martin, G. R. *J. Natl. Cancer Inst.* **1986**, *77*, 311−316.

(2) (a) Liotta, L. A. *Cancer Res.* **1986**, *46*, 1−7. (b) Liotta, L. A.; Rao, C. N.; Wewer, U. M. *Annu. Rev. Biochem.* **1986**, *55*, 1037−1057.

(3) (a) Blood, C. H.; Zetter, B. R. *Biochim. Biophys. Acta* **1990**, *1032*, 89−118. (b) Folkman, J.; Shing, Y. *J. Biol. Chem.* **1992**, *267*, 10931−10934. (c) Weinstat-Saslow, D.; Steeg, P. S. *FASEB J.* **1994**, *8*, 401−407.

(4) (a) Koretz, K.; Schlag, P.; Boumsell, L.; Moller, P. *Am. J. Pathol.* **1991**, *138*, 741−750. (b) Damjanovich, L.; Albelda, S. M.; Mette, S. A.; Buck, C. A. *Am. J. Respir. Cell. Mol.* **1992**, *6*, 197−206. (c) Natali, P. G.; Nicotra, M. R.; Botti, C.; Mottolese, M.; Bigotti, A.; Segato, O. *Br. J. Cancer* **1992**, *66*, 318−322. (d) Zutter, M. M.; Krigman, H. R.; Santoro, S. A. *Am. J. Pathol.* **1993**, *142*, 1439−1448.

(5) (a) Albeda, S. M.; Motto, S. A.; Elder, D. E.; Stewart, R. M.; Damjanovich, L.; Herlyn, M.; Buck, C. A. *Cancer Res.* **1990**, *50*, 6757−6764. (b) Gladson, C. L.; Cheresh, D. A. *J. Clin. Invest.* **1991**, *88*, 1924−1932.

(6) Brooks, P. C.; Clark, R. A. F.; Cheresh, D. A. *Science* **1994**, *264*, 569−571.

(7) (a) Wayner, E. A.; Carter, W. G. *J. Cell Biol.* **1987**, *105*, 1873−1884. (b) Cheresh, D. A.; Spiro, R. G. *J. Biol. Chem.* **1987**, *36*, 17703−17711. (c) Humphries, M. J.; Yamada, K. M.; Olden, K. *J. Clin. Invest.* **1988**, *81*, 782−790. (d) Gehlsen, K. R.; Argraves, W. S.; Pierschbacher, M. D.; Ruoslathi, E. *J. Cell Biol.* **1988**, *106*, 925−930.

(8) Brooks, P. C.; Montgomery, A. M. P.; Rosenfeld, M.; Reisfeld, R. A.; Hu, T.; Klier, G.; Cheresh, D. A. *Cell* **1994**, *79*, 1157−1164.

(9) (a) Ruoslahti, E.; Pierschbacher, M. D. *Science* **1987**, *238*, 491−497. (b) D'Souza, S. E.; Ginsberg, M.; Plow, E. *Trends Biochem. Sci.* **1991**, *16*, 246−250. (c) Albeda, S. M.; Buck, C. A. *FASEB J.* **1990**, *4*, 2868−2880. (d) Hynes, R. O. *Cell* **1987**, *48*, 549−554.

S0002-7863(96)00372-1 CCC: $12.00

chirality.[10,11] This procedure led to the highly $\alpha_V\beta_3$-active and selective cyclic pentapeptides *cyclo*(-Arg-Gly-Asp-D-Phe-Val-) and *cyclo*(-Arg-Gly-Asp-Phe-D-Val-).[10] The D-Phe-containing peptide also suppresses tumor-induced angiogenesis in a chick chorioallantoic membrane (CAM) model.[8]

Strategy

Investigations of a variety of linear and cyclic RGD-peptides showed that additional amino acids influence the activity of the RGD-containing sequence toward the $\alpha_{IIb}\beta_3$ receptor. In particular, hydrophobic amino acids following the aspartic acid increase the activity.[12]

Here we present SAR investigations under "conformational control"[13] on the influence of the amino acids at positions 4 and 5 in the structurally defined cyclic pentapeptide system *cyclo*(-Arg^1-Gly^2-Asp^3-Xxx^4-Yyy^5-) on the activity and selectivity of the inhibition of vitronectin binding to the isolated $\alpha_V\beta_3$ receptor. Therefore, either Phe or Val of the two first-generation peptides *cyclo*(-Arg-Gly-Asp-D-Phe-Val-) (lead structure I; **LS1**) and *cyclo*(-Arg-Gly-Asp-Phe-D-Val-) (lead structure II; **LS2**) was replaced by a variety of hydrophobic and hydrophilic, natural and unnatural amino acids. The resulting peptides can be divided into four distinct conformational classes with defined structures (Figure 1).

Classes 1 and 2 differ from 3 and 4 in the position of the structure-inducing D-amino acid. In classes 1 and 2 the D-amino acid is in position 4 of the cyclic peptides. In peptides of classes 3 and 4 the D-amino acid appears in position 5.

Cyclic pentapeptides often show a βII′/γ-turn arrangement where the D-amino acid occupies the $i + 1$ position of the βII′-turn.[10,14] Therefore, the position of Arg^1 is expected to be the $i + 3$ position of the βII′-turn in classes 1 and 2 and to be the $i + 2$ position of the βII′-turn in classes 3 and 4.

The second distinguishing feature is the position of the variable amino acid. In classes 1 and 3, position 4 and, in classes 2 and 4, position 5 are screened with the described set of amino acids, while the other position is unvaried.

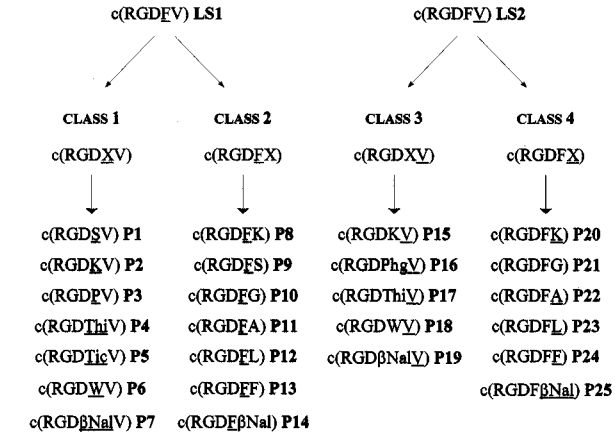

Figure 1. Classification of the different peptides. Common amino acids are abbreviated using the usual one letter code. D-configuration is indicated by underlining. Non-natural amino acids are abbreviated as follows: β-(2-naphthyl)-alanine (βNal), phenylglycine (Phg), β-(2-thienyl)alanine (Thi), 1,2,3,4-tetrahydroisochinoline carbonic acid (Tic). The ranking of the peptides within the different classes is carried out according to the increasing hydrophobicity determined by HPLC retention times.

For each class at least one hydrophilic amino acid and a series of hydrophobic, aliphatic, and aromatic amino acids were employed.

Results

Conformation. The discussion of the structural behavior of the peptides under "conformational control"[13] is based on the assumption that within each different class the peptides possess structural homogeneity. This homogeneity can be verified by comparing experimental parameters like H^N-, H^α-, and $^{13}C^\alpha$-chemical shift data, temperature coefficients of the H^N-shifts, coupling constants, and NOE-derived interproton distances. This strategy is demonstrated for the peptides of class 3.

The similarity in the H^N-, H^α-, and $^{13}C^\alpha$-shifts (Figure 2), which are sensitive to conformational changes, as well as the resemblance of the temperature coefficients (Table 1), gives the first hints for the consistent structural behavior within this class. Only peptide **P16**, which contains phenylglycine, shows larger differences in the chemical shift data. This can be attributed to anisotropy effects of the phenyl group which is directly bonded to the α-carbon and, therefore, close to the backbone atoms in discussion.

Besides this simple evidence the most obvious method to show similarity is the direct comparison of the ^3J-coupling constants and NOE-derived interproton distances, which determine the structure of the peptides. These data show good agreement for all peptides within class 3 (see Tables 1B and 2).

Distance geometry calculations using NOE-derived distances as well as *J*-coupling restraints were done for each member of class 3 to verify our statement of the structural homogeneity within the different classes on the basis of experimental parameters. A superposition of the backbone atoms is exhibited in Figure 3.

The analysis of the chemical shift data, the temperature coefficients, the coupling constants, and the interproton distances of classes 1, 2, and 4 reveals analogous results (data not shown). Within classes 1 and 2 all peptides show comparable experimental data. Only the peptides c(RGDPV) (**P3**) and c(RGDTicV) (**P5**) of class 1 differ from the average values (details see below).

On the basis of these results only one representative member of each class (c(RGDKV) (**P2**) for class 1, c(RGDFK) (**P8**) for

(10) (a) Gurrath, M.; Müller, G.; Kessler, H.; Aumailly, M.; Timpl, R. *Eur. J. Biochem.* **1992**, *210*, 911−921. (b) Müller, G.; Gurrath, M.; Kessler, H.; Timpl, R. *Angew. Chem.* **1992**, *104*, 341−343; *Angew. Chem., Int. Ed. Engl.* **1992**, *31*, 326−328. (c) Aumailly, M.; Gurrath, M.; Müller, G.; Calvete, J.; Timpl, R.; Kessler, H. *FEBS Lett.* **1991**, *291*, 50−54. (d) Pfaff, M.; Tangemann, B.; Müller, B.; Gurrath, M.; Müller, G.; Kessler, H.; Timpl, R.; Engel, J. *J. Biol. Chem.* **1994**, *269*, 20233−20238. (e) Haubner, R.; Gurrath, M.; Müller, G.; Aumailley, M.; Kessler, H. *Prospects in Diagnosis and Treatment of Breast Cancer. Proceedings of the Joint International Symposium on Prospects in Diagnosis and Treatment of Breast Cancer*, 10−11 November 1993, Munich; Schmitt, M., Graeff, H., Kindermann, G., Eds.); Elsevier Science Publishers, B.V.: Amsterdam, The Netherlands, 1994.

(11) (a) Kessler, H.; Gratias, R.; Hessler, G.; Gurrath, M.; Müller, G. *Pure Appl. Chem.* **1996**, *68*, 1201−1205. (b) Kessler, H.; Diefenbach, B.; Finsinger, D.; Geyer, A.; Gurrath, M.; Goodman, S. L.; Hölzemann, G.; Haubner, R.; Jonczyk, A.; Müller, G.; Graf v. Roedern, E.; Wermuth, J. *Lett. Pept. Sci.* **1995**, *2*, 155−160.

(12) (a) Barker, P. L.; Bullens, S.; Bunting, S.; Burdick, D. J.; Chan, K. S.; Deisher, T.; Eigenbrot, C.; Gadek, T. R.; Gantzos, R.; Lipari, M. T.; Muir, C. D.; Napier, M. A.; Pitti, R. M.; Padua, A.; Quan, C.; Stanley, M.; Struble, M.; Tom, J. Y. K.; Burnier, J. P. *J. Med. Chem.* **1992**, *35*, 2040−2048. (b) Cook, N. S.; Kottirsch, G.; Zerwes, H.-G. *Drugs Future* **1994**, *19*, 135−159. (c) Cheng, S.; Craig, W. S.; Mullen, D. G.; Tschopp, J. F.; Pierschbacher, M. D. *J. Med. Chem.* **1994**, *37*, 1−8. (d) Gould, R. J. *Perspect. Drug Discovery Design* **1994**, *1*, 537−548.

(13) Kessler, H.; Gemmecker, G.; Haupt, A.; Klein, M.; Wagner, K.; Will, M. *Tetrahedron* **1988**, *44*, 745−759.

(14) (a) Demel, D.; Kessler, H. *Tetrahedron Lett.* **1976**, 2801−2804. (b) Kessler, H.; Hölzemann, G. *Liebigs Ann. Chem.* **1981**, 2028−2044. (c) Kessler, H.; Kutscher, B. *Tetrahedron Lett.* **1985**, *26*, 177−180. (d) Stroup, A. N.; Rockwell, A. L.; Gierasch, L. M. *Biopolymers* **1992**, *32*, 1713−1725. (e) Coles, M.; Sowemimo, V.; Scanlon, D.; Munro, S. L.; Craik, D. J. *J. Med. Chem.* **1993**, *36*, 2658−2665. (f) Bean, J. W.; Peishoff, C. E.; Kopple, K. D. *Int. J. Pept. Protein Res.* **1994**, *44*, 223−232.

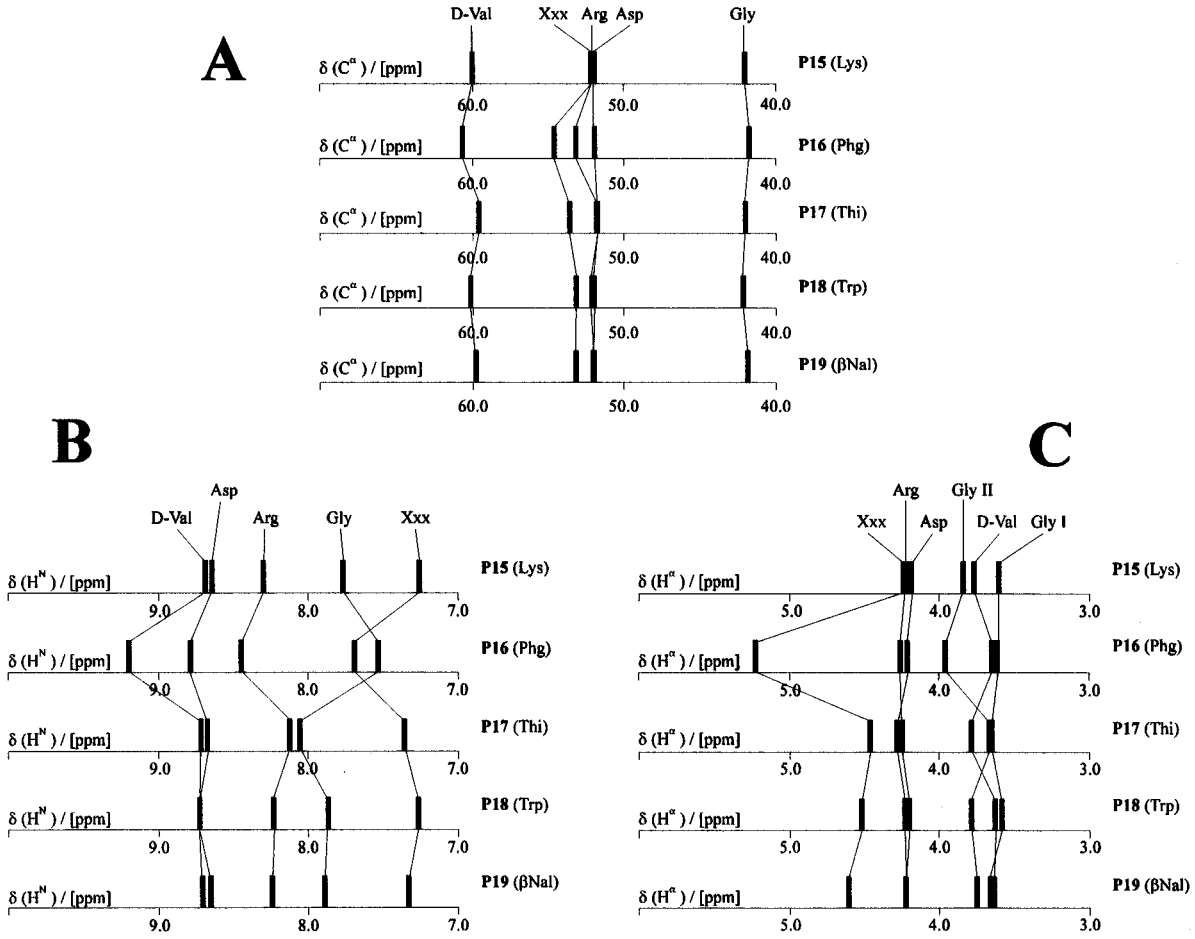

Figure 2. Analysis of the C^{α}- (A), H^{N}- (B), and H^{α}-chemical shift data (C) giving the first indications of the structural homogeneity within class 3.

Table 1. Data for the Peptides of Class 3 c(RGDXV) in DMSO

(a) Temperature Dependence of the Amide Protons with the Coefficients Given in Negative Parts per Billion per K

no.	peptide	Arg[1]	Gly[2]	Asp[3]	Xxx[4]	D-Val[5]
P15	c(RGDKV)	7.9	0.3	6.1	0.3	9.7
P16	c(RGDPhgV)	7.3	-0.4	2.4	0.6	6.4
P17	c(RGDThiV)	4.6	2.3	6.3	0.2	7.4
P18	c(RGDWV)	6.6	1.0	5.1	-0.7	7.9
P19	c(RGDβNalV)	5.7	1.1	6.0	0.0	6.0

(b) Proton Vicinal Coupling Constants $^{3}J(H^{N},H^{\alpha})$ (Hz) at 300 K

no.	peptide	Arg[1]	Gly[2]	Asp[3]	Xxx[4]	D-Val[5]
P15	c(RGDKV)	8.5	7.4/3.6	6.6	8.0	7.4
P16	c(RGDPhgV)	8.6	8.0/3.3	6.5	8.0	7.4
P17	c(RGDThiV)	8.8	6.9/4.5	6.9	7.4	7.7
P18	c(RGDWV)	8.9	7.4/3.7	6.9	7.5	7.4
P19	c(RGDβNalV)	8.7	7.2/[a]	6.7	7.8	7.6

[a] Coupling constants could not be measured.

Table 2. Comparison of H^{N}/H^{N}- and H^{N}/H^{α}-Distances (pm) of Class 3 Peptides

distances between atoms	P15 (Lys)	P16 (Thi)	P17 (Phg)	P18 (Trp)	P19 (βNal)
$Arg^{1}HN-Gly^{2}HN$	276		255	264	297
$Arg^{1}HN-Val^{5}HN$	406	349	386		372
$Gly^{2}HN-Asp^{3}HN$	378	357	347		356
$Gly^{2}HN-Xxx^{4}HN$	320	348			352
$Gly^{2}HN-Val^{5}HN$			442		
$Asp^{3}HN-Xxx^{4}HN$	246	249	240	237	264
$Xxx^{4}HN-Val^{5}HN$	357	352	376		365
$Arg^{1}HN-Arg^{1}H^{\alpha}$	283		282	281	
$Arg^{1}HN-Val^{5}H^{\alpha}$	212	217		212	231
$Gly^{2}HN-Arg^{1}H^{\alpha}$	287		286	289	
$Gly^{2}HN-Gly^{2}H^{\alpha h}$	266				
$Gly^{2}HN-Gly^{2}H^{\alpha}$	271				
$Gly^{2}HN-Gly^{2}H^{\alpha}$				251	285
$Asp^{3}HN-Gly^{2}H^{\alpha}$	285				
$Asp^{3}HN-Gly^{2}H^{\alpha h}$	216				
$Asp^{3}HN-Gly^{2}H^{\alpha}$		211	247	245	
$Asp^{3}HN-Asp^{3}H^{\alpha}$	285	291	284	273	
$Xxx^{4}HN-Gly^{2}H^{\alpha}$	331	339	354	426	
$Xxx^{4}HN-Asp^{3}H^{\alpha}$		320	324	291	
$Xxx^{4}HN-Xxx^{4}H^{\alpha}$	264	285	278		292
$Val^{5}HN-Xxx^{4}H^{\alpha}$	219	220	210	215	236
$Val^{5}HN-Val^{5}H^{\alpha}$	282	289		270	301

class 2, c(RGDKV) (**P15**) for class 3, and c(RGDFK) (**P20**) for class 4) was chosen for a detailed structure determination. The discussion of the SAR is based on these representative peptides. In addition to the structures of these four peptides from the different classes, the two peptides containing Trp (c(RGDWV) (**P6**) and c(RGDWV) (**P18**)), and the two compounds **P3** (c(RGDPV)) and **P5** (c(RGDTicV), which show differences in the above-mentioned parameters compared with the rest of the peptides of class 1, were also calculated.

Class 1: *cyclo*(-Arg-Gly-Asp-D-Xxx-Val-). A rough inspection of the experimental NMR parameters (see Supporting Information) immediately indicates that class 1 peptides can be divided into two subclasses. The two peptides **P3** (containing D-Pro) and **P5** (containing D-Tic), both with a tertiary amide bond between the aspartic acid and the D-amino acid, are significantly different from the other members of this class. In particular, the chemical shift data and the temperature coefficients of the arginine H^{N} exhibit distinct characteristic differences, e.g. the H^{N}-resonances of **P3** and **P5** are shifted to lower field by about 1 ppm, and the temperature coefficients of the

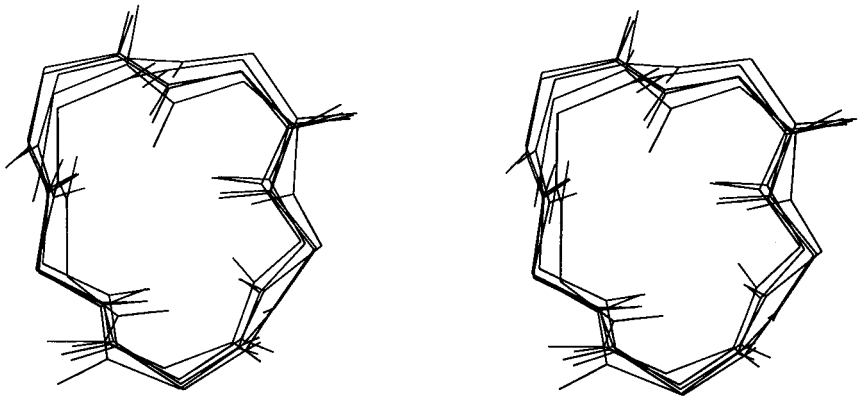

Figure 3. Stereoplot of the superimposed backbone conformations of the five class 3 peptides. Structures resulting from DG calculations.

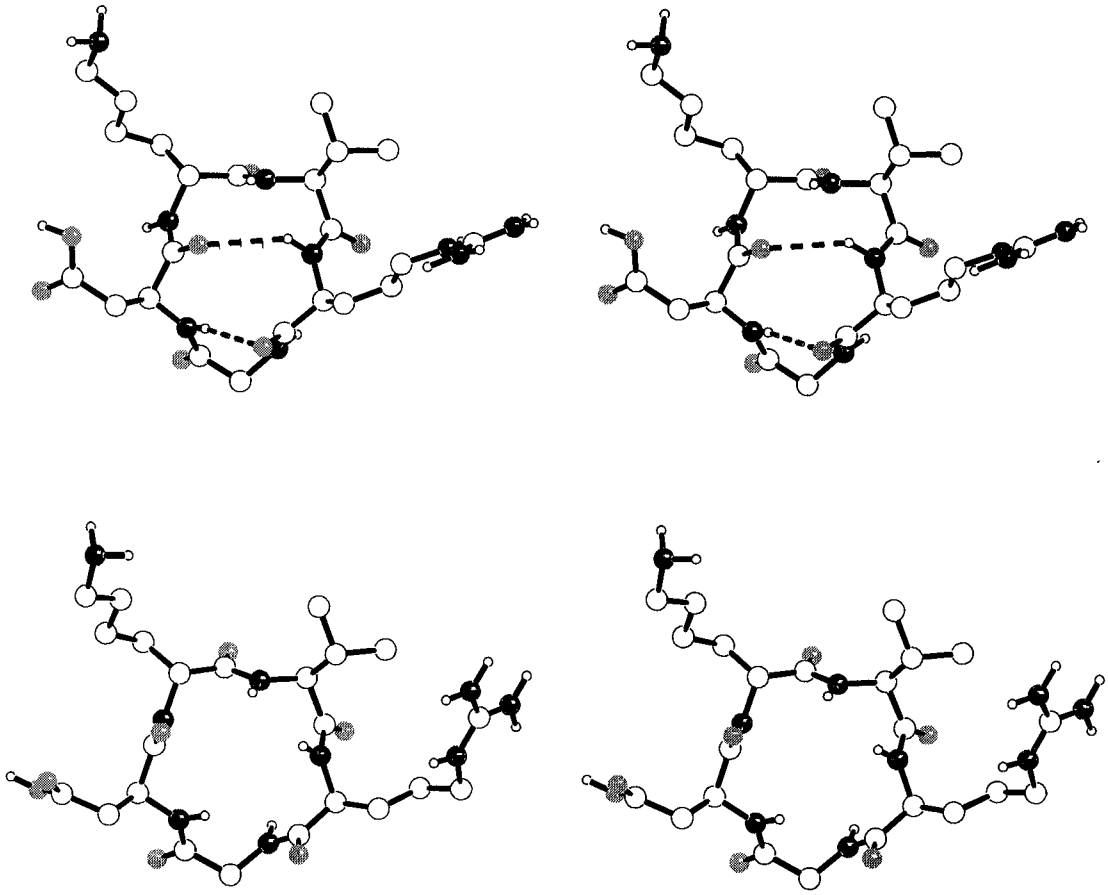

Figure 4. Stereoplot of the averaged and minimized structures **P2/MD1** (at the top) and **P2/MD2** (at the bottom) from the restrained MD simulation of c(RGDK̲V) (**P2**). Large circles show carbon (open), oxygen (gray), and nitrogen (black) atoms. Polar hydrogen atoms are indicated by small circles. Hydrogen bonds stabilizing the βII′- and γ-turn are indicated by dashed lines.

arginine amide protons of **P3** and **P4** are significantly larger (−10.0 and −7.6 ppb/K, respectively) than those of the remaining peptides of class 1 (about −1.8 ppb/K). Therefore, additional structure investigations of these two peptides were performed.

In general, a βII′/γ-turn arrangement is expected for the backbone of class 1 cyclopeptides, in which the variable D-amino acid occupies the $i + 1$ position of the βII′-turn and glycine the $i + 1$ position of the γ-turn. Careful analysis of the restrained MD trajectory of peptide **P2**, in DMSO, shows that the Arg−Gly and the Gly-Asp peptide bonds can flip between two different conformations.

This phenomenon is typical for cyclic pentapeptides of this kind. Small but still significant NOE's were usually observed between the amide protons of Arg and Gly. The origin of this effect could be elucidated by ensemble calculations[15] which show conformational dynamics in the region of the γ-turn.

The averaged structure **P2/MD1**, obtained from the trajectory between 20 and 40 ps, is in good agreement with the expected βII′/γ-turn conformation (Figure 4) whereas the second averaged structure **P2/MD2**, which corresponds to the trajectory between 60 and 95 ps, exhibits no typical secondary structural elements (Figure 4).

The major difference between these two conformations is the orientation of the amide bond between Asp[3] and D-Lys[4]. In **P2/MD2** the amide bond is nearly perpendicular to the plane of the ring, preventing the carbonyl oxygen from participating

(15) Mierke, D. F.; Kurz, M.; Kessler, H. *J. Am. Chem. Soc.* **1993**, *116*, 1042−1049.

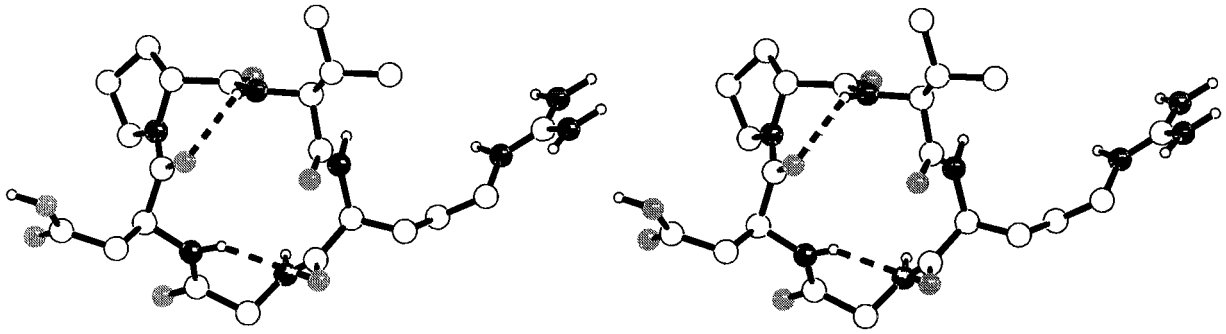

Figure 5. Stereoplot of the averaged and minimized structures resulting from restrained MD simulation of c(RGDPV) (**P3**). Large circles show carbon (open), oxygen (gray), and nitrogen (black) atoms. Polar hydrogen atoms are indicated by small circles. Hydrogen bonds stabilizing the γ-turns are indicated by dashed lines.

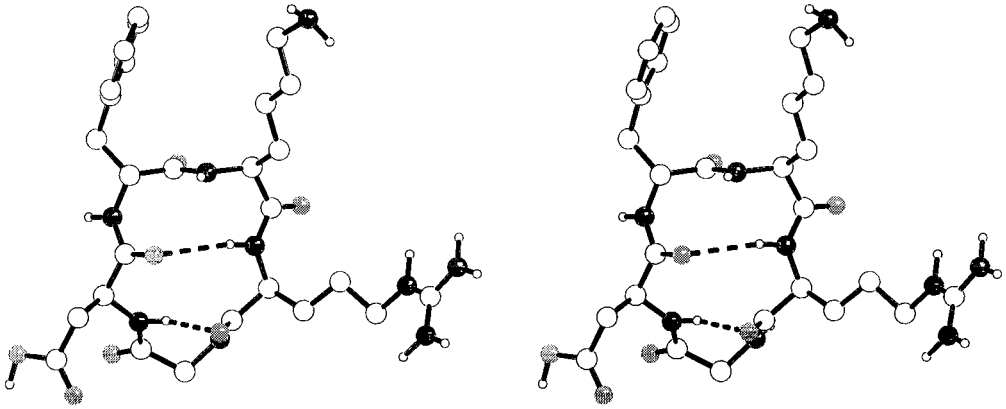

Figure 6. Stereoplot of the averaged and minimized structure resulting from MD simulations of c(RGDFK) (**P8**). Large circles show carbon (open), oxygen (gray), and nitrogen (black) atoms. Polar hydrogen atoms are indicated by small circles. Hydrogen bonds stabilizing the βII′- and γ-turn are indicated by dashed lines.

in a hydrogen bond to the Arg^1H^N. The length of the "hydrogen bond" in the γ-turn region is also larger than usual.

Besides this flip in the MD trajectory there is additional evidence for the flexible behavior of cyclic pentapeptides of this type: all temperature coefficients of the amide protons are in the range -3 to -4 ppb/K. As strong differences in the temperature dependence of the amide proton shifts indicate conformational preference, the absence of these differences suggests flexible behavior.

Another criterion for flexibility is the agreement of distances calculated from MD simulations and NOE-derived intermolecular distances.[16] In flexible regions it is normally not possible to achieve good agreement between these variables within the time scale of MD simulations. In our case, the distances of the averaged MD structures in the region of the γ-turn ($Arg^1H^N-Gly^2H^N$, $Gly^2H^N-Asp^3H^N$) are too short by about 50 pm, which exceeds the error of the measurement. Due to the r^{-6}-dependence of the NOE, short distances in minor populated conformations can contribute significantly to the observed values. Similar problems occur with the ^3J-coupling constants, which are in much better agreement for **P2/MD1** than for **P2/MD2**.

Nevertheless, since most of the dynamical behavior concerns rotations of the amide bonds, the orientation of the pharmacophoric side chains (e.g. the arginine or the aspartic acid C^α/C^β vectors) is very similar in both conformations and, therefore, only **P2/MD1** is taken into account for the discussion of the SAR below.

Similar results have been obtained from the calculations for peptide **P6** (*cyclo*(-Arg-Gly-Asp-D-Trp-Val-)) (see Supporting Information). The identical results for both peptides **P2** and **P6** confirm the similarity of the structures within the same class.

Substitution of the D-amino acid by D-Pro or D-Tic (**P3** and **P5**) yields stronger conformational effects. For peptide **P3** (*cyclo*(-Arg-Gly-Asp-D-Pro-Val-)) the minimization of the structure, averaged over 100 ps (20−120 ps) of the MD trajectory, reveals a γ/γ-turn pattern with Gly^2 and D-Pro^4 in the two $i+1$ positions. In addition, a distorted βI′-turn with Arg^1 in the $i+1$ position is observed. But altogether the experimental data for peptide **P3** favor the conformation with two γ-turns (Figure 5).

A similar conformation with Gly^2 and D-Tic^4 in the $i+1$ position of the two γ-turns is found for *cyclo*(-Arg-Gly-Asp-D-Tic-Val-) (**P5**). The violations in the region of Gly^2, by analogy with the other members of class 1, can be explained by a flexible amide bond between Arg^1 and Gly^2. But altogether the D-Pro- and D-Tic-containing peptides seem to be more rigid than the rest of class 1. Obviously, this is due to the Φ-angle restriction and the additional restricted side chain orientation in these two amino acids. In accordance with these observations the temperature coefficients of these two peptides are more differentiated.

Class 2: *cyclo*(-Arg-Gly-Asp-D-Phe-Xxx-). In contrast to the observation for class 1 peptides, the experimental data are very similar for all class 2 peptides and give evidence for conformational preference. The peptide **P8** (*cyclo*(-Arg-Gly-Asp-D-Phe-Lys-)), which was chosen as a representative member of this class, shows the expected βII′/γ-conformation with D-Phe^4 in the $i+1$ position of the βII′-turn and Gly^2 in the $i+1$ position of the γ-turn (Figure 6).

The averaged, minimized structure also corresponds with experimental ^3J-coupling and all NOE-derived distance data.

(16) Kessler, H.; Bats, J. W.; Lautz, J.; Müller, A. *Liebigs Ann. Chem.* **1989**, 913−928.

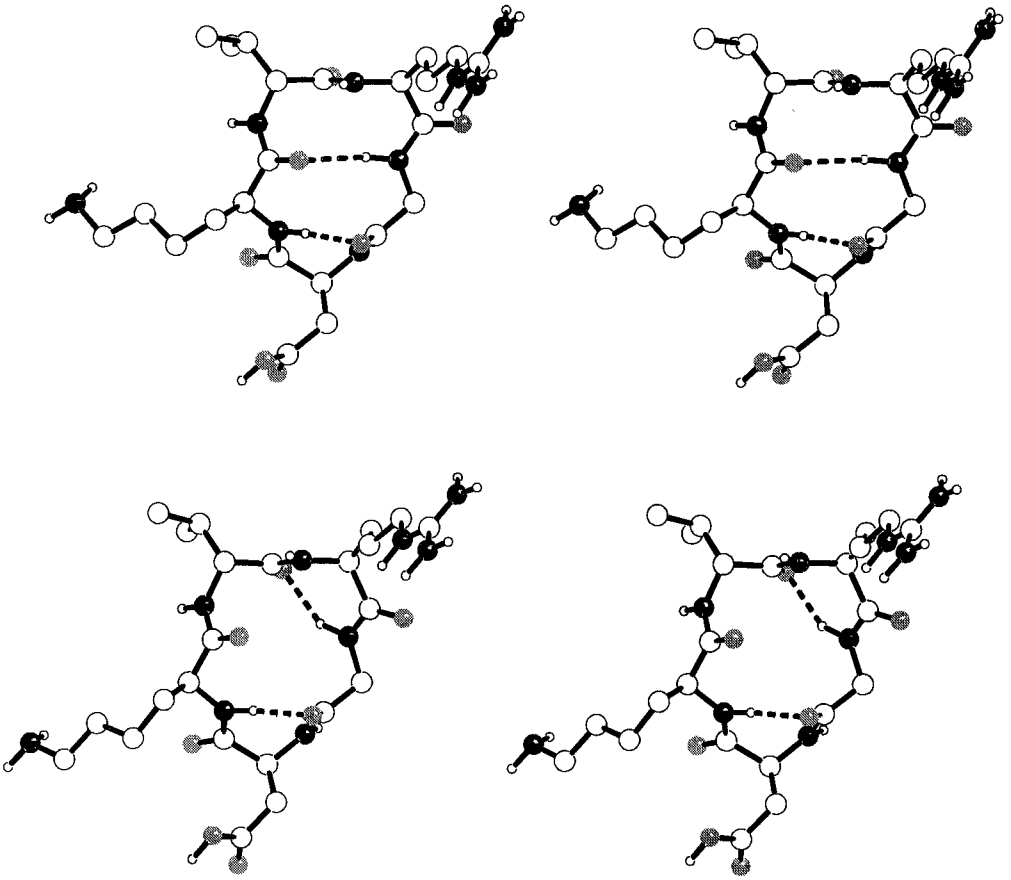

Figure 7. Stereoplot of the averaged and minimized structures **P15/MD1** (at the top) and **P15/MD2** (at the bottom) from the restrained MD-simulation of c(RGDKV) (**P15**). Large circles show carbon (open), oxygen (gray), and nitrogen (black) atoms. Polar hydrogen atoms are indicated by small circles. Hydrogen bonds stabilizing the βII′-, γ-, and γ_i-turn are indicated by dashed lines.

Only the upper bound of two backbone NOE restraints is slightly violated. One of these violations (Arg^1H^N/Gly^2H^N) is typical for the previously mentioned flexibility in the γ-turn region in cyclic pentapeptides.[15] The other violation (Arg^1H^N/Lys^5H^α), by analogy with class 1, indicates a slightly flexible amide bond between residues 5 and 1. This flexibility may explain the relatively small differences in the temperature coefficients of the amide protons. Only Arg^1H^N is totally shielded from the solvent (-1.3 ppb/K). The other four coefficients between -2.8 and -5.3 ppb/K are in the mean range and indicate amide bond ϕ, ψ-flexibility.

Class 3: *cyclo*(-Arg-Gly-Asp-Xxx-D-Val-). To be comparable to the other classes, the Lys-containing peptide **P15** was chosen for further refinement by MD simulation in solvent. By analogy with the two previously described classes, the peptide **P15** exhibits flexible amide bonds which result in two different conformations during the simulation.

The first one (**P15/MD1**), which is stable between 38 and 79 ps, shows the expected βII′/γ-turn pattern with D-Val^5 in the $i + 1$ position of the β-turn (Figure 7). The main difference in the second structure, **P15/MD2** (80−150 ps), is a flipped amide bond between Arg^1 and Gly^2. This flip of about 50° destroys the βII′-turn and results in the formation of a γ^i-turn with Arg^1 in the $i + 1$ position (Figure 7). The experimental temperature coefficients (low temperature dependence of Gly^2H^N and Lys^4H^N chemical shifts) of the amide protons as well as most of the NOE and ^3J-coupling data are in good agreement with both conformations. However, the short Arg^1H^N/Gly^2H^N NOE distance (276 pm) especially confirms the assumption that **P15/MD1** might be a better representation of the experimental data. The backbone NOE-restraints, which are violated in both conformations (Asp^3H^N/Lys^4H^N, Asp^3H^N/Asp^3H^α), are in the region of the flexible γ-turn with Asp^3 in the $i + 1$ position.

Class 4: *cyclo*(-Arg-Gly-Asp-Phe-D-Xxx-). According to the design principle, class 4 should exhibit similar conformations to those of class 3: a βII′/γ-turn pattern with the variable amino acid D-Xxx^5 in the $i + 1$ position of the β-turn and Asp^3 in the γ-turn-like region. Since the experimental data from each member of class 4 are similar, the lysine-containing peptide **P20** (*cyclo*(-Arg-Gly-Asp-Phe-D-Lys-)) was chosen for structure determination. Surprisingly, this peptide reveals a shifted βII′/γ-turn pattern with Gly^2 in the $i + 1$ position of the β-turn instead of the D-amino acid D-Lys^5 (Figure 8).

An analogous pattern was previously found for other *cyclo*(-Xxx-Gly-Xxx-Xxx-D-Yyy-) peptides like *cyclo*(-Pro-Gly-Pro-Ser-D-Ala-).[17] Nevertheless, the averaged, minimized structure corresponds with the experimental data. Only one upper boundary (Arg^1H^N/Gly^2H^N) is violated, which, by analogy with the discussion above, is interpreted as a peptide bond flip of the Arg^1/Gly^2 amide bond.

Biological Data

The ability of cyclic pentapeptides to inhibit the binding of vitronectin and fibrinogen to the isolated $\alpha_{IIb}\beta_3$ and $\alpha_V\beta_3$ receptor was compared with that of the linear standard peptide GRGDSPK and with those of the lead structures c(RGDFV) (**LS1**) and c(RGDFV) (**LS2**). Inhibitory peptides were able to fully suppress the binding of ligands to the isolated receptors, and the binding kinetics followed a classic sigmoid path. In absolute terms, linear GRGDSPK blocked vitronectin binding

(17) Karle, I. L. *J. Am. Chem. Soc.* **1979**, *101*, 181−184.

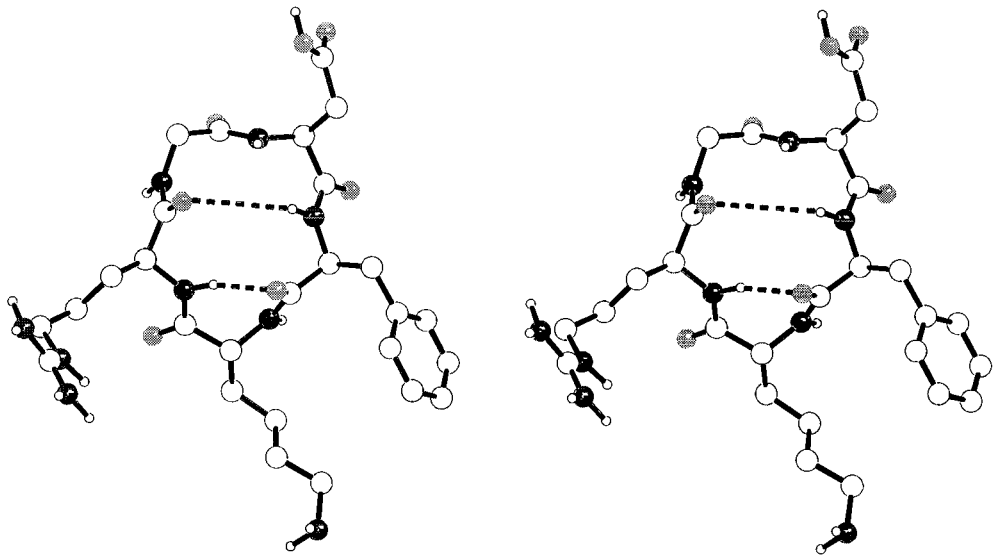

Figure 8. Stereoplot of the averaged and minimized structure resulting from MD simulations of c(RGDFK) (**P20**). Large circles show carbon (open), oxygen (gray), and nitrogen (black) atoms. Polar hydrogen atoms are indicated by small circles. Hydrogen bonds stabilizing the βII′- and γ-turn are indicated by dashed lines.

to $\alpha_V\beta_3$ with an IC_{50} of 1.2 ± 0.27 μM (SEM: $n = 26$) and to $\alpha_{IIb}\beta_3$ with an IC_{50} of 5.4 ± 2.0 μM (SEM: $n = 26$). For c(RGDFV) (**LS1**) the IC_{50} values were 4.9 ± 0.1 nM (SEM: $n = 22$) and 1.7 ± 0.38 μM (SEM: $n = 22$), respectively. To obtain intra-assay comparable results, we introduce normalized activities given as the ratio $Q = IC_{50}$[peptide]/IC_{50}[GRGDSPK]. Only these Q-values are used for further discussions.

In the case of the $\alpha_V\beta_3$ receptor, all peptides except for c(RGDPV) (**P3**) are more active than the standard peptide GRGDSPK. The strongest antagonist c(RGDβNalV) (**P7**) shows a 1000-fold higher activity compared with that of the standard peptide and is about 6 times more active than the lead structure **LS1** (c(RGDFV)). Besides **P7** most of the remaining peptides also show potent activity with Q-values in the range of 10^{-3}. Only peptides **P2** and **P15** with lysine as well as peptides **P3** and **P5** with an *N*-alkylated cyclic D-amino acid (D-Pro, D-Tic) in position 4 have weak inhibitory abilities.

On the other hand, all cyclic pentapeptides show only moderate or low activities when used to inhibit fibrinogen binding to the $\alpha_{IIb}\beta_3$ receptor. The most active peptides are about 10- to 20-fold more active than the standard peptide. The lowest activities are obtained for the peptides **P2**, **P8**, and **P15** with lysine, the peptides **P10** and **P12** with glycine or leucine, respectively, and the peptides **P3** and **P5** with D-Pro or D-Tic, respectively. These activities are 10 to 50 times lower than the activity of the linear standard peptide.

Peptides of classes 3 and 4 show only moderate selectivity for the $\alpha_V\beta_3$ receptor. They inhibit vitronectin binding to $\alpha_V\beta_3$ up to 50-fold more strongly than fibrinogen binding to $\alpha_{IIb}\beta_3$. On the other hand, there are highly selective compounds among the peptides of classes 1 and 2, which inhibit vitronectin binding to the $\alpha_V\beta_3$ receptor up to 7500-fold better than fibrinogen binding to the $\alpha_{IIb}\beta_3$ receptor. The peptide with the highest selectivity is c(RGDβNalV) (**P7**) followed by the peptides **P10** and **P12**, which are about 3500-times more active in blocking the vitronectin$-\alpha_V\beta_3$ interaction compared with the fibrinogen$-\alpha_{IIb}\beta_3$ interaction.

Discussion

Conformational Aspects. Cyclic peptides still have a considerable mobility of their backbone. Recently, we pointed out the similarity of the conformational behavior of cyclic pentapeptides with all trans peptide bonds and cyclopentane.[11a] To understand the conformational behavior of these peptides, one has to consider that the α-carbon atoms generally form an envelope-type conformation in which the four α-carbons of the βII- or βII′-turn are in one plane. This requires that not all four can be L-configurated. Normally, in a βII′-turn the amino acid in the $i + 1$ position has D-configuration or is glycine. Amide bond orientation between these α-carbons has a strong tendency to avoid 1,3-allylic strain between the carbonyl oxygen and the β-carbon or the next carbonyl group. Hence, in most cases the atoms $O-C-N-C^{\alpha}-H$ lie cis in one plane. It is important to note that stabilization via intramolecular hydrogen bonds does not contribute to a large extent to the backbone structure.[18]

The high flexibility of this "cyclopentane-like" conformations also finds its expression in the side chain conformational equilibrium. It is, therefore, difficult to draw definitive conclusions about the bioactive conformation.

The number and array of amino acid chirality determines the preferred conformation. The inducing effect of a D-amino acid in the $i + 1$ position of a βII′-turn is often stated; indeed, this secondary structure element is found in almost all peptides discussed here (Gly often also acts as a D-amino acid). In a βII′-turn the amide proton of the amino acid in the $i + 2$ position is close to the carbonyl oxygen in position i. The latter often forms bifurcated hydrogen bonds to the amino group of the amino acid in the $i + 2$ (γ-turn) and $i + 3$ positions (βII′-turn). Slight changes in backbone dihedral angles therefore switch the structure from βII′/γ- to γ/γ-arrangements (differences between an ideal βII′- and γ-turn: $\Delta\Phi_{i+1} = 10°$, $\Delta\Psi_{i+1} = -60°$).

Another phenomenon is the flipping of trans amide bonds in the γ-turn region. This motion often occurs in cyclic peptides.[16,19] In cyclic pentapeptides these kinds of dynamics were proven by ensemble calculations.[15]

For a SAR discussion, the dynamic nature of constrained peptides has to be taken into account. As stated long ago (see e.g. ref. 20), the structure formed by the double induced fit of the receptor and the substrate cannot be derived directly from

(18) Snyder, J. P. *J. Am. Chem. Soc.* **1984**, *106*, 2393−2400.
(19) Romanowska, K.; Kopple, K. D. *Int. J. Pept. Protein Res.* **1987**, *30*, 289−298.
(20) Kessler, H. *Angew. Chem.* **1982**, *94*, 509−520; *Angew. Chem., Int. Ed. Engl.* **1982**, *21*, 512−526.

the most stable conformation in solution. However, the restriction of the conformational space in connection with biological activities give a hint for optimizing structural requirements. This restriction was, in our case, achieved by the use of small cyclic pentapeptides containing one D-amino acid.

For a structural comparison, the differences between classes 1/2 and 3/4 must be taken into account. In classes 1 and 2 the resulting β-turn with the D-amino acid in the $i + 1$ position was found in most peptides. Only the structures containing the *N*-alkylated amino acids D-Pro and D-Tic (**P3** and **P5**) prefer the γ-turn in the region of the D-amino acid. In classes 3 and 4 the D-amino acid was also expected to prefer the $i + 1$ position of the βII′-turn. This arrangement, however, was observed only for class 3 peptides. The peptides of class 4 reveal a different βII′/γ-turn pattern with glycine in the $i + 1$ position of the βII′-turn, shifting the D-amino acid into the $i + 1$ position of the γ-turn. This effect is a consequence of the special sequential order with glycine in position 2 and the D-amino acid in position 5 of the cyclic pentapeptide *cyclo*(-Xxx-Gly-Xxx-Xxx-D-Yyy-). It seems that for this special arrangement both conformations are energetically equivalent. However, the conformation of class 4 peptides with the D-amino acid in the γ-turn seems to be preferred, because both the glycine and the D-amino acid occupy favorable positions in the cyclic pentapeptide template. The contradictory behavior of class 3 peptides could be explained by the steric requirements of the valine side chain, which does not fit well in the $i + 1$ position of a γ-turn.

As stated above, another interesting point is the flexibility within these small cyclic peptides. Most of the peptides show high flexibility in the backbone. The strongest effects result from motions of the amide bond planes. Some of these flips and/or vibrations can be detected during the MD simulations (e.g. the flips of the amide bond between the $i + 2$ and $i + 3$ positions of the β-turn-like structure). The mobility of the γ-turn region in the βII′/γ-turn pattern is much more difficult to detect. Exchange between two or more conformations in this region could not be found in restrained MD calculations but was confirmed by additional ensemble calculations using ensemble-averaged NOE-derived distances and ^3J-coupling restraints (see Supporting Information). The violation of some H^N-H^N−NOE effects can therefore only be explained by a dynamic process, fast on the NMR time scale but slow on the time scale of the calculation. Since in all four peptide classes these motions have no strong influence on the relative orientation of the C^α/C^β vectors of the pharmacophoric groups, they can be neglected for the structure−activity correlation discussion.

Structure−Activity Relationships

Influence of the Variable Amino Acid on the Biological Activity of the Peptides. A variety of amino acids with different hydrophobic or hydrophilic side chains within the four classes were synthesized. Since conformational analysis demonstrates that the backbone conformations within the classes are almost the same according to the principle of "conformational control",[13] we note that the different activities observed within the classes are determined mainly by the different side chain functionalities and not by conformational differences. Structural aspects are taken into account only for peptides **P3** and **P5** of class 1, which show distinct conformational differences.

At first glance, in class 1 there seems to be no discernible tendency for the $\alpha_V\beta_3$ receptor inhibition, but neglecting **P3** and **P5** (different structure, see above), peptide **P2** with the hydrophilic D-lysine in position 4 inhibits both receptors only weakly. In comparison to **P2**, the peptides **P4**, **P6**, **P7**, and **LS1**, with hydrophobic side chains, possess very high inhibitory activities on the vitronectin−$\alpha_V\beta_3$ interaction.

Analogous results are found for the peptides of class 3. The hydrophilic substitution in position 4 (**P15**) results in weak activities on both receptors, whereas all hydrophobic aromatic replacements (**P16**−**P19** and **LS2**) result in enhanced activity (Figure 9). These findings suggest that a hydrophobic amino acid in position 4 increases the activity for both receptors independently from the different structural requirements of the two peptidic classes.

By contrast, the high activity of c(RGDSV) (**P1**) with D-serine in position 4 cannot result from hydrophobic interactions. The side chain hydroxyl group might form a hydrogen bond with an acceptor group of the receptor in addition to the hydrophobic interactions that also take place in this region. More studies have to be done to verify this interpretation.

Classes 2 and 4 are characterized by the variation of the amino acid in position 5. The inhibitory activities on the vitronectin−$\alpha_V\beta_3$ interactions of both class 2 and class 4 show no dependency on the polarity of the variable amino acid: hydrophobic as well as hydrophilic replacements reveal similar activities within the peptides of both classes. Concerning the $\alpha_{IIb}\beta_3$ receptor, the activities of the peptides within class 4 are independent of the variations of the amino acids, whereas for class 2 the peptides **P9**, **P11**, **P13**, **P14**, and **LS2** show 30- to 150-times higher activities than **P8**, **P10**, and **P12**. However, among the latter peptides there are hydrophobic as well as hydrophilic amino acid substitutions; hence, no obvious correlation between hydrophilicity and activity exists (Figure 9).

Recently, Healy et al.[21] investigated peptide ligands for the $\alpha_V\beta_3$ integrin from random phage display libraries. With few exceptions, the study considered only qualitative binding to $\alpha_V\beta_3$: there is no quantitative correlation between activity and the flanking amino acids. Among the peptides for which binding assays were done, derivatives with two cysteines flanking the RGD-motif which are disulfide bridged exhibit the strongest binding to $\alpha_V\beta_3$. These findings suggest that a partial rigidity introduced by disulfide bonding may aid high-affinity binding to $\alpha_V\beta_3$ and, therefore, support our approach of using conformationally constrained peptides.

Influence of the Amide Proton of the Amino Acid in Position 4. Superposition of the two different structures found for class 1 peptides (depicted for peptides **P3** and **P6**, Figure 10) shows that the only notable difference in the two conformations is the orientation of the amide bond between Val^5 and Arg^1. But the motion of this bond has almost no influence on the orientation of the C^α/C^β vectors of the pharmacophoric groups of the RGD-sequence, which are mainly responsible for activity (Figure 10). Furthermore, in the most active peptides of classes 1 and 2, the proton of this amide bond is involved in an intramolecular hydrogen bond and thus is hardly accessible for receptor interactions. Therefore, the drastic loss of inhibitory activity of **P3** and **P5** on vitronectin−$\alpha_V\beta_3$ interaction cannot be ascribed to conformational changes. In addition, the amide proton of the arginine is known to be not essential for high inhibitory activities on $\alpha_{IIb}\beta_3$.[22]

(21) Healy, J. M.; Murayama, O.; Maeda, T.; Yoshino, K.; Sekiguchi, K.; Kikuchi, M. *Biochemistry* **1995**, *34*, 3948−3955.

(22) (a) Ali, E. F.; Bennett, D. B.; Calvo, R. R.; Elliot, J. D.; Hwang, S.-M.; Ku, T. W.; Lago, M. A.; Nichols, A. J.; Romoff, T. T.; Shah, D. H.; Vasko, J. A.; Wong, A. S.; Yellin, T. O.; Yuan, C. K.; Samanen, J. M. *J. Med. Chem.* **1994**, *37*, 769−780. (b) Jackson, S.; DeGrado, W. F.; Dwivedi, A.; Pathasarathy, A.; Higley, A.; Krywko, J.; Rockwell, A.; Markwalder, J.; Wells, G.; Wexler, R.; Mousa, S.; Harlow, R. *J. Am. Chem. Soc.* **1994**, *116*, 3220−3230.

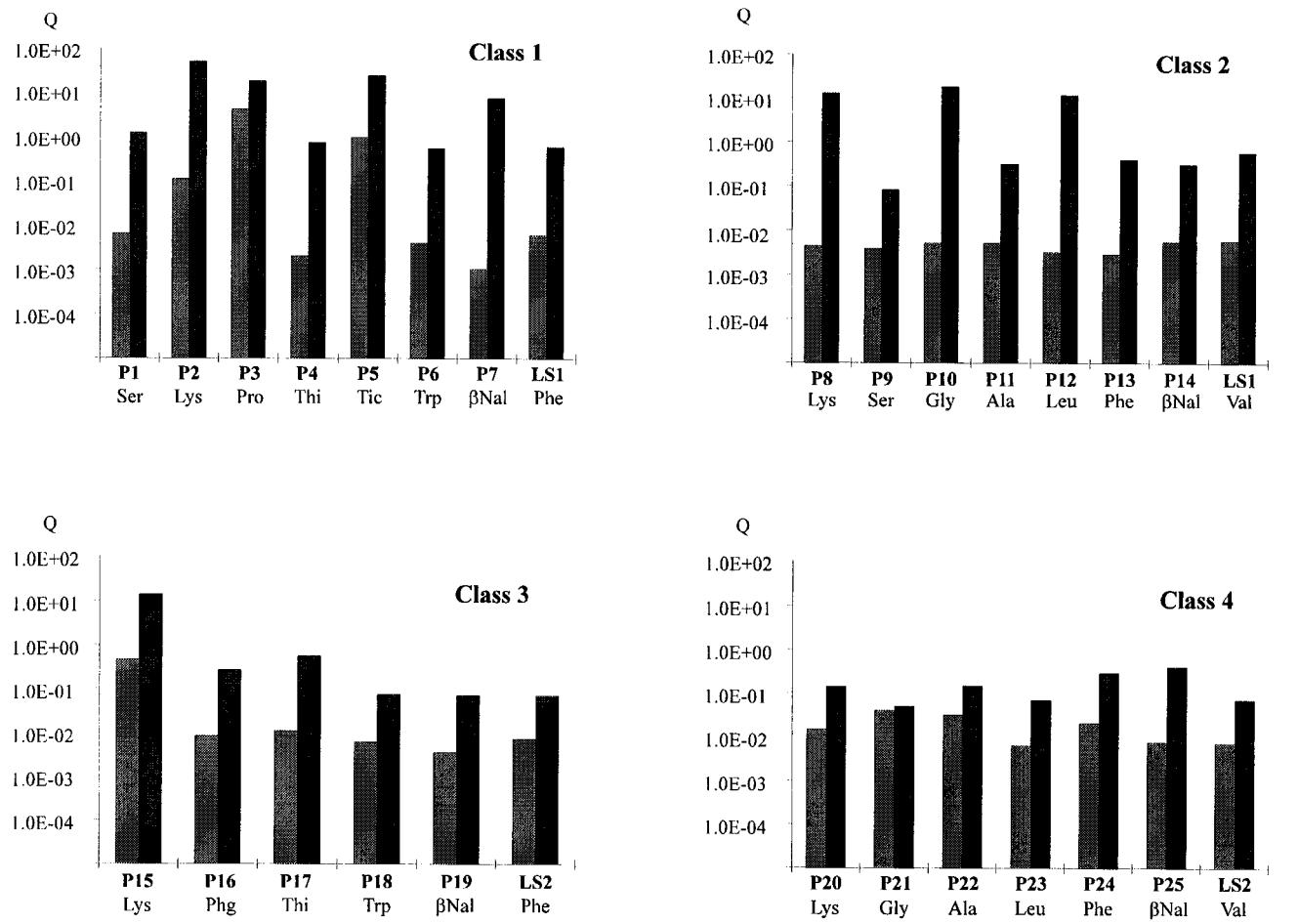

Figure 9. Comparison of the activities of the four different classes: class 1, c(RGDXV); class 2, c(RGDFX); class 3, c(RGDXV); class 4, c(RGDFX). Values are given as relative activities $Q = IC_{50}$[peptide]/IC_{50}[GRGDSPK]. Coding: $\alpha_V\beta_3$, light gray; $\alpha_{IIb}\beta_3$, dark gray.

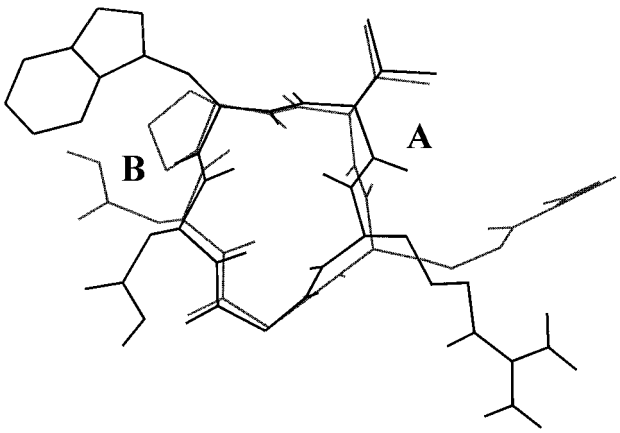

Figure 10. Structural differences of the peptides **P2**/**P6** (subfamily 1) and **P3**/**P5** (subfamily 2) of class 1 shown using the superposition of peptide **P6** (black) and **P3** (gray): **A**, different orientation of the amide bond between Val^5 and Arg^1; **B**, the amino acid in position 4 of **P3** (D-Pro) possesses no amide proton.

One reason for the low activity of c(RGDPV) (**P3**) could be the loss of the hydrophobic side chain in position 4. Therefore c(RGDTicV) (**P5**) with the aromatic isoquinoline group could be more active compared with **P3** if the orientation of the phenyl ring matches the steric and electronic demands of the receptor. But this is not observed. Besides their similar conformations, both peptides have another common feature which could explain their low activities: D-Pro^4 of **P3** as well as D-Tic^4 of **P5** possesses no amide proton. This proton seems to be essential for high activities especially for the inhibition of vitronectin binding to the $\alpha_V\beta_3$ receptor, because for $\alpha_{IIb}\beta_3$ no such behavior is observed. Here the activities of **P3** and **P5** are in the same range as those of other peptides within this class like **P2** and **P7** (Figure 9).

This postulated formation of a hydrogen bond between the proton of the amide bond between residues 3 and 4 and an acceptor within the receptor might also explain the somewhat higher activities of class 1 and 2 peptides compared with the analogous peptides of classes 3 and 4. The amide proton in residue 4 of the peptides of classes 1 and 2 (with the exceptions of **P3** and **P5**) is exposed to solvent and, therefore, orientated in a way suitable for interaction with a hydrogen bond acceptor in the receptor. By contrast, the amide hydrogen of the same residue in the peptides of classes 3 and 4 is involved in an intramolecular hydrogen bond and is thus orientated toward the center of the peptide ring (Figure 11). For the formation of an intermolecular hydrogen bond, rotation of the amide bond must occur, with negative influence on activity. In addition, investigations on *N*-methylated RGD-peptides show that the methylation of the amide bond between Asp^3 and the following amino acid also reduces activity.[23] Furthermore, structure−activity investigations on cyclic peptide analogues[24] provide results which also confirm the importance of this amide proton for the high activity of the inhibition of vitronectin binding to $\alpha_V\beta_3$.

Structural Differences of the Four Peptide Classes. At first glance, the activities of the peptides of the four classes in

(23) Unpublished results.
(24) Haubner, R.; Schmitt, W.; Hölzemann, G.; Goodman, S. L.; Jonczyk, A.; Kessler, H. *J. Am. Chem. Soc.*, submitted.

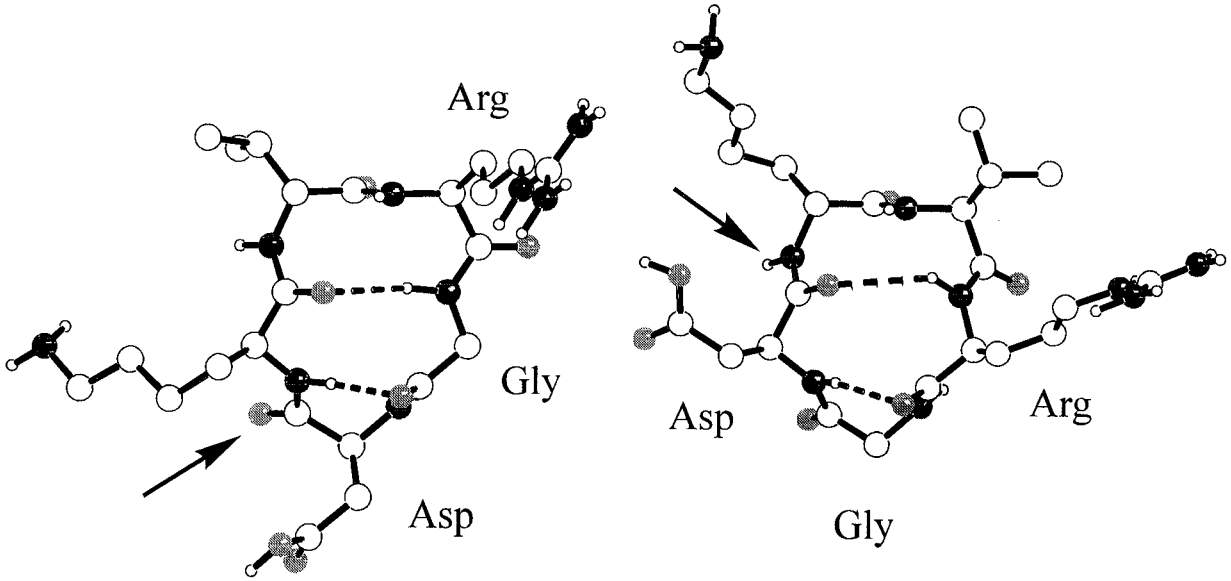

Figure 11. Different orientation of the proton of the amide bond (indicated by an arrow) between Asp[3] and residue 4 in classes 1 and 2 and classes 3 and 4 demonstrated by **P2** (right side) and **P15** (left side).

inhibiting vitronectin binding to $\alpha_V\beta_3$ show no distinct differences (exceptions: peptides **P2**, **P3**, **P5**, and **P15**). The weak inhibitory capacities of these four are not attributable to conformational influences but to the lysine side chain for **P2** and **P15** and the missing amide proton of residue 4 for **P3** and **P5**. The remaining peptides have *Q*-values in the range 10^{-2} to 10^{-3}.

Comparing the activities of two peptides with the same sequence but with the D-amino acid in a different location and, therefore, with different conformations (e.g. c(RGDThiV) (**P4**) of class 1 with a *Q*-value of 1.1×10^{-2} and c(RGDThiV) (**P17**) of class 3 with a *Q*-value of 2.0×10^{-3}), the peptide with the D-amino acid in position 4 always shows a somewhat higher activity than the peptide with the D-amino acid in position 5. This suggests that the conformations of the peptides of classes 1 and 2 with the D-amino acid in position 4 fit slightly better into the receptor pocket than the peptides of classes 3 and 4.

The analysis of the differences in the selectivities between peptides of classes 1 and 3 and peptides of classes 2 and 4 with similar sequences shows analogous results. The selectivity of the peptides with the D-amino acid in postion 4 (classes 1 and 2) is always higher than those of the peptides with the D-amino acid in position 5 (classes 3 and 4).

Superposition of the representative conformations of the four classes shows that the main structural differences are focused on the distance between the C^α-atom of the arginine and the C^α-atom of the aspartic acid and the corresponding C^β/C^β-distances,[25] as well as the orientation of the amide bond between residues 3 and 4 (see above and Figure 12). The C^α/C^α-distances are in the range of 520 pm for the peptides of classes 1 and 2, 600 pm for the peptides of class 4, and 675 pm for class 3 peptides. The C^β/C^β-distances are about 710 pm for the peptides of classes 1 and 2, about 850 pm for class 4 peptide and about 900 pm for the peptides of class 3. The orientations of the pharmacophoric groups relative to one other, characterized by the angles μ(Arg), ν(Asp), and the dihedral φ (for definition see also ref 25) (Table 3) are almost the same for all four classes. This result shows that in the peptides of classes 1 and 2 the RGD-sequence is in a bent conformation (γ-turn with Gly[2] in the $i + 1$ position) and in the peptides of classes 3 and 4 it is in a more elongated conformation. The elongated conformation seems to be slightly more unfavorable for binding to the $\alpha_V\beta_3$ receptor. The peptides of classes 3 and 4 with the elongated conformation can also fit in the $\alpha_{IIb}\beta_3$ receptor, whereas the peptides of classes 1 and 2 with the bent RGD-conformation bind with high affinity only to $\alpha_V\beta_3$ and much more weakly to $\alpha_{IIb}\beta_3$.

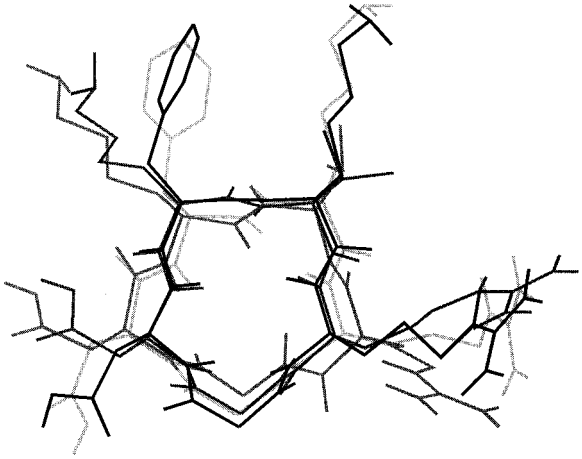

Figure 12. Superposition of the structures of the representative peptides of class 1 (black), class 2 (dark gray), class 3 (light gray), and class 4 (gray).

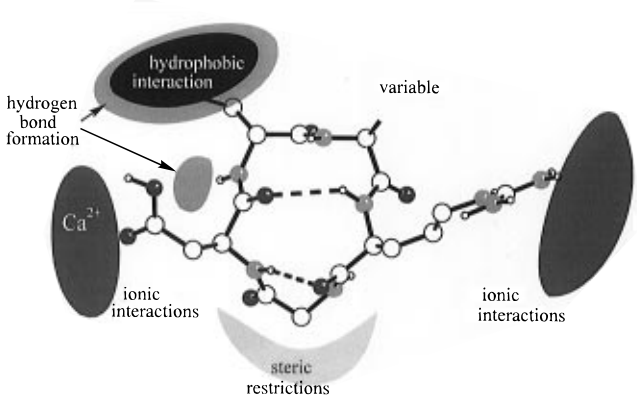

Figure 13. Receptor model summarizing our results in combination with earlier findings.

(25) Müller, G.; Gurrath, M.; Kessler, H. *J. Comput. Aided Mol. Des.* **1994**, *8*, 709−730.

Table 3. Characterization of the Relative Orientation of the Biologically Relevant RGD-Sequence[a]

no. (class)	peptide	C^{α}/C^{α} [b] (pm)	C^{β}/C^{β} [c] (pm)	μ(Arg)[d]	ν(Asp)[e]	φ[f]
P2 (1/1)[g]	c(RGDKV)	531	694	127°	118°	−7°
P6 (1/1)	c(RGDWV)	518	713	138°	122°	−11°
LS1 (1/1)	c(RGDFV)	512	744	139°	139°	+5°
P8 (2)	c(RGDFK)	511	701	130°	128°	+8°
P3 (1/2)[h]	c(RGDPV)	551	780	152°	129°	−4°
P5 (1/2)	c(RGDTicV)	541	778	146°	135°	−6°
P15 (3)	c(RGDKV)	689	892	127°	118°	+1°
P18 (3)	c(RGDWV)	645	872	156°	125°	+1°
LS2 (3)	c(RGDFV)	658	905	139°	144°	−15°
P20 (4)	c(RGDFK)	605	840	150°	132°	+13°

[a] For definition of the parameters used, see also ref 25. [b] Distance between the C^{α}-atoms of Arg[1] and Asp[3]. [c] Distance between the C^{β}-atoms of Arg[1] and Asp[3]. [d] Angle built of $C^{\beta}-C^{\alpha}$(Arg) vector and C^{α}(Arg)$-C^{\alpha}$(Asp) vector. [e] Angle built of $C^{\beta}-C^{\alpha}$(Asp) vector and C^{α}(Asp)$-C^{\alpha}$(Arg) vector. [f] dihedral built of $C^{\alpha}-C^{\beta}$ vectors of Arg and Asp. [g] Subfamilie 1 of class 1, characterized by a βII′/γ-turn arrangement. [h] Subfamilie 2 of class 1, characterized by a γ/γ-turn arrangement.

However, these points require further study, for the high flexibility of the cyclic pentapeptides certainly also allows larger conformational changes during receptor binding.

The very high selectivtiy of the peptides **P7**, **P8**, **P10**, and **P12**, which are about 3000- (**P8**) to 7500-times (**P7**) more active in the inhibition of vitronectin binding to $\alpha_V\beta_3$ than in fibrinogen binding to $\alpha_{IIb}\beta_3$, reflects the comparatively low activities of these peptides in inhibiting $\alpha_{IIb}\beta_3$. These distinctly low activities are not explicable by conformational effects, because the peptides show no structural behavior which distinguishes them from the remaining peptides of classes 1 and 2 (excluding **P3** and **P5**: not taken into account here).

Conclusion

The conformational analyses of the individual peptides of classes 2−4 reveal similar backbone structures within the different classes. Class 1 is divided into two subclasses.

All peptides examined are more-or-less flexible, mainly due to motions of the amide bonds. However, this flexibility has almost no influence on the relative position of the C^{α}-atoms to each other or on the orientation of the C^{α}/C^{β} vectors of the pharmacophoric groups.

The SAR investigations show that an hydrophobic aromatic amino acid in position 4 increases the activity for the $\alpha_V\beta_3$ receptor. However, the hydrophilic amino acid serine also increases inhibitory activity. Thus, hydrophobic interactions as well as the formation of hydrogen bonds in the region of position 4 must be considered. By contrast, neither hydrophobic nor hydrophilic substitutions in position 5 influence the activity. This position is thus valuable as a target for molecular and functional modifications.[10d] In addition, the proton of the amide bond between Asp[3] and residue 4 seems to be important for strong inhibition of vitronectin$-\alpha_V\beta_3$ interaction. Only peptides which possess an amide proton that can form a hydrogen bond with the receptor show very high activities. Furthermore a more bent conformation of the RGD-sequence with ArgC^{α}/AspC^{α}-distances of about 500 pm and ArgC^{β}/AspC^{β}-distances of about 700 pm fits better in the $\alpha_V\beta_3$ receptor than in the $\alpha_{IIb}\beta_3$ receptor. This conformational preference is also reflected in high selectivities among the peptides of classes 1 and 2.

Our experiments lead to an improved $\alpha_V\beta_3$ ligand-binding model and give new insight into the structural requirements of this receptor: they contribute to our understanding of integrin−ligand interactions. Moreover, we have discovered highly active and selective $\alpha_V\beta_3$ antagonists: IC_{50}'s in the nanomolar range complement a 3- to 4-orders of magnitude higher activity for $\alpha_V\beta_3$ than for $\alpha_{IIb}\beta_3$. In future, these compounds and their structural relatives will be prospective candidates for drug development targeting specific $\alpha_V\beta_3$ interactions, including tumor metastasis, angiogenesis, acute renal failure, and osteoporosis.

Experimental Section

Peptide Synthesis. The peptides were synthesized by solid phase peptide synthesis[26] using the *o*-chlorotrityl chloride resin[27] applying a Fmoc strategy.[28] The final Fmoc protection group was removed with 20% piperidine in DMF. The peptide was cleaved from the resin using a mixture of acetic acid, TFE, and DCM (1:1:3). Cyclization was performed via *in situ* activation using diphenylphosphorylazide with sodium bicarbonate as solid base[29] under high dilution conditions. For side chain deprotection the cyclic peptide was treated with a solution of 85.5% TFA, 5% phenol, 2% water, 5% thioanisole, and 2.5% ethanedithiol. All peptides were characterized by FAB mass spectrometry, amino acid analysis, and various NMR techniques (see Supporting Information).

NMR Spectroscopy. Total correlated spectroscopy (TOCSY)[30] was used for proton assignments, and heteronuclear multiple-quantum coherence (HMQC),[31] for carbon assignment. The sequential assignment of proton resonances was achieved by nuclear Overhauser enhancement and exchange spectroscopy (NOESY)[32] or rotating frame nuclear Overhauser enhancement and exchange spectroscopy (ROESY).[33] Chemical shift data can be found in the Supporting Information.

Quantitative information on interproton distances for the structure determination was obtained from analyzing NOESY or ROESY spectra with mixing times of 150 and 180 or 200 ms, respectively. For correct conversion of measured ROESY integral volumes into corresponding distances, the offset effect was taken into account.[34] For all distance calculations, the isolated two-spin approximation[35] was used. Interproton distances and homonuclear coupling constants were employed as constraints for subsequent structure calculations[36] (for details see Supporting Information).

Structure Calculation. For the structure calculations two different procedures were used. Most of the structures were calculated by combining distance geometry methods with restrained molecular dynamics. For distance geometry, a modified version[36] of the program DISGEO[37] was used. Further restrained MD refinement was done with the program GROMOS.[38] For the peptides **P2** and **P3** the high-temperature molecular dynamics approach was applied to search the conformational space. To explore the dynamic properties of the peptides, in analogy to similar work on a model cyclic pentapeptide,[15]

(26) (a) Merrifield, R. B. *J. Am. Chem. Soc.* **1963**, *85*, 2149−2154. (b) Merrifield, R. B. *Angew. Chem.* **1985**, *97*, 801−812; *Angew. Chem., Int. Ed. Engl.* **1985**, *24*, 799−810.

(27) (a) Barlos, K.; Gatos, D.; Kallitsis, J.; Papahotiu, G.; Sotiriu, P.; Wenqing, Y.; Schäfer, W. *Tetrahedron Lett.* **1989**, *30*, 3943−3946. (b) Barlos, K.; Chatzi, O.; Gatos, D.; Stavropoulos, G. *Int. J. Pept. Protein Res.* **1991**, *37*, 513−520.

(28) (a) Carpino, L. A. *J. Am. Chem. Soc.* **1970**, *92*, 5748−5749. (b) Fields, G. B.; Noble, R. L. *Int. J. Pept. Protein Res.* **1990**, *35*, 161−214.

(29) Brady, S. F.; Paleveda, W. J.; Arison, B. H.; Freidinger, R. M.; Nutt, R. F.; Veber, D. F. An improved procedure for peptide cyclization. In *Peptides: Structure and Function.* Proceedings of the 8th American Peptide Symposium; Hruby, V. J., Rich, D. H., Eds.; Pierce Chemical Company: Rockford, IL, 1983; pp 127−130.

(30) (a) Braunschweiler, L.; Ernst, R. R. *J. Magn. Reson.* **1983**, *52*, 521−528. (b) Bax, A.; Byrd, R. A.; Aszlos, A. *J. Am. Chem. Soc.* **1984**, *106*, 7632−7633.

(31) Müller, L. *J. Am. Chem. Soc.* **1979**, *101*, 4481−4484.

(32) (a) Jeener, J.; Meier, B. H.; Bachmann, P.; Ernst, R. R. *J. Chem. Phys.* **1979**, *71*, 4546−4553. (b) Wüthrich, K. *NMR of proteins and nucleic acids*; Wiley: New York, 1986.

(33) (a) Bothner-By, A. A.; Stephensen, R. L.; Lee, J.; Warren, C. D.; Jeanloz, R. W. *J. Am. Chem. Soc.* **1984**, *106*, 811−813. (b) Kessler, H.; Griesinger, C.; Kerssebaum, R.; Wagner, K.; Ernst, R. R. *J. Am. Chem. Soc.* **1987**, *109*, 607−609.

(34) Griesinger, C.; Ernst, R. R. *J. Magn. Reson.* **1987**, *75*, 261−271.

(35) Neuhaus, D.; Williamson, M. *The Nuclear Overhauser Effect in Structural and Conformational Analysis*; VCH: Weinheim, Germany, 1989.

(36) Mierke, D. F.; Kessler, H. *Biopolymers* **1993**, *33*, 1003−1017.

an ensemble calculation of 400 structures was carried out with the peptide **P18**. More detailed information about the different calculation protocols and the used experimental data can be found in the Supporting Information.

Integrin Ligand Binding and Competition Assays. Protein purification has been detailed elsewhere.[39] Human extracellular matrix ligand (ECM ligand) vitronectin was purified from plasma by heparin−Sepharose affinity chromatography,[40] and fibrinogen was purified from whole blood by gel filtration.[41] Human integrin $\alpha_V\beta_3$ was purified from term placenta by LM609−antibody affinity chromatography.[42] Human integrin $\alpha_{IIb}\beta_3$ was purified from outdated platelets by GRGDSP−peptide affinity chromatography.[43] Protein concentrations were estimated against a BSA standard curve with the BCA method (Pierce).

For the isolated integrin−ligand binding assay ECM ligands were labeled by biotinylation. Integrins diluted to 1 μg/mL (∼1:1000 dilution of stock) were adsorbed to 96-well nontissue culture treated microtitre plates. After blocking of free protein binding sites biotinylated ECM ligand at 1 μg/mL was added and incubation continued at 30 °C for 3 h. Unbound ligand was washed away and bound biotin detected with alkaline-phosphate-conjugated anti-biotin antibodies.[44] For peptide competition assays, peptides were serially diluted before addition to integrin-coated wells, followed by co-incubation with biotinylated ligand and detection as described above. Assays were performed in triplicate, the mean binding values were fitted to a sigmoid, and the IC_{50} was derived. Values shown represent the mean of at least three separate determinations of IC_{50}.

External standards of linear GRGDSPK and c(RGDfV) were routinely included to monitor the dynamic range and the stability of the assay.

Acknowledgment. Financial support by the Deutsche Forschungsgemeinschaft and the Fonds der Chemischen Industrie is gratefully acknowledged. R.G. thanks the Studienstiftung des Deutschen Volkes for the fellowship. The authors thank Dr. J. Winkler for contributing some FAB-mass spectra; M. Kranawetter, B. Cordes, and M. Wurl for HPLC separations; and Dr. B. Felding-Habermann for assistance in the early phase of the establishment of the biological test system.

Supporting Information Available: Additional tables with ^{1}H- and ^{13}C-chemical shift data for all 25 peptides, selected homonuclear ^3J-coupling constants, and for **P18** additional heteronuclear ^3J-coupling constants, temperature coefficients of all peptides, comparisons between experimentally determined and simulated NOE-derived distances of all calculated peptides, and analytical data such as FAB-masses, data from amino acid analysis, HPLC retention times, and yields of the peptides as well as quantitative biological activity data. Protocols of the DG/MD calculations, additional stereoplots of the peptides **P5**, **P6**, and **P18**, and detailed information about experimental conditions are also included (altogether 37 pages). See any current masthead page for ordering and Internet access instructions.

JA9603721

(37) (a) Havel, T. F. DISGEO, Quantum Chemistry Exchange Program, Exchange No. 507, Indiana University, 1988. (b) Havel, T. F. *Prog. Biophys. Mol. Biol.* **1991**, *56*, 43−78. (c) Crippen, G. M.; Havel, T. F. *Distance Geometry and Molecular Conformation*; Research Studies Press LTD., John Wiley & Sons: Somerset, England, 1988. (d) Havel, T. F.; Wüthrich, K. *Bull. Math. Biol.* **1984**, *46*, 673−698.

(38) (a) van Gunsteren, W. F.; Berendsen, H. J. C. Groningen Molecular Simulations (GROMOS) Library Manual. *GROMOS user manual*; Biomos B. V.: Nijenborgh 16 NL 9747 AG Groningen, 1987. (b) Hermans, J.; Berendsen, H. J. C.; van Gunsteren, W. F.; Postma, J. P. M. *Biopolymers* **1984**, *23*, 1513−1518. (c) van Gunsteren, W. F.; Berendsen, H. J. C. *Angew. Chem.* **1990**, *102*, 1020−1055; *Angew. Chem., Int. Ed. Engl.* **1990**, *29*, 992−1023.

(39) Mitjans, F. C.; Sander, D.; Adán, J.; Sutter, A.; Martinez, J. M.; Jäggle, C.; Moyano, J. M.; Kreysch, H.; Piulats, J.; Goodman, S. L. *J. Cell Sci.* **1995**, *108*, 2825−2838.

(40) Yatohgo, T.; Izumi, M.; Kashiwagi, H.; Hayashi, M. *Cell Struct. Funct.* **1988**, *13*, 281−292.

(41) Kazal, L. A.; Ansel, S.; Miller, O. P.; Tocantins, L. M. *Proc. Soc. Exp. Biol. Med.* **1963**, *113*, 989−994.

(42) Smith, J. W.; Cheresh, D. A. *J. Biol. Chem.* **1988**, *263*, 18726−18731.

(43) Pytela, R.; Pierschbacher, M. D.; Ginsberg, M. H.; Plow, E. F.; Ruoslahti, E. *Science* **1986**, *231*, 1559−1562.

(44) Smith, J. W.; Vestal, D. J.; Irwin, S. V.; Burke, T. A.; Cheresh, D. A. *J. Biol. Chem.* **1990**, *265*, 11008−11013.